On the Scheme Dependency of the Three-Dimensional Euler Solutions

By

Yoko TAKAKURA*, Tomiko ISHIGURO** and Satoru OGAWA**

(February 5, 1987)

1. INTRODUCTION

Owing to startling progress of recent computers and numerical analysis methods, three-dimensional flows about bodies have been solved without difficulty. Until the present, various difference schemes have been developed for solving the Euler equations, and the recent remarkable progress in numerical technique is the development of TVD schemes proposed by Yee & Harten [1] and by Chakravarthy & Osher [2]. Numerical experiments in one dimensional flow problems show these schemes have the high resolution capabilities for shock waves and give satisfactory solutions in even rough grids. However, their numerical experiments of two-dimensional flows have been successfully carried out in only fine grids for a few cases. The availabilities of schemes for multi-dimensional problems in general coordinates, where number of grid points is not still enough and the change of metrics in coordinate direction is large, can be estimated only through practical calculations.

In the present study, first we three-dimensionalize both the TVD schemes and modify the Yee-Harten TVD scheme with regard to treatment of metrics and the Chakravarthy-Osher TVD scheme according to their similar suggestion. Next we solve the Euler equations for three-dimensional flows about the ONERA-M6 wing by using these TVD schemes and the conventional Beam-Warming scheme [3], and compare the solutions by the three schemes with the experimental data. As a result, our modification are proved to be reasonable and it is indicated that the solutions by both the original TVD schemes are smeared with the unconsidered differentials of metrics. Moreover it is made sure through practical calculations that the smear due to disagreement of accuracy between metrics and fluxes is removed by maintaining freestream [11]. Further the characteristic feature of the TVD schemes in general three-dimensional coordinate systems becomes clearly evident through computations for two typical patterns of flowfield.

2. GOVERNING EQUATIONS

The three-dimensional Euler equations in Cartesian coordinates

* Scientific Systems Department, Fujitsu Limited
** Computer Center, National Aerospace Laboratory

$$\partial_t Q+\partial_x E+\partial_y F+\partial_z G=0,$$

are transformed into the conservation law in general curvilinear coordinates

$$\partial_\tau \hat{Q}+\partial_\xi \hat{E}+\partial_\eta \hat{F}+\partial_\zeta \hat{G}=0,$$

with a transformation of variables

$$\tau=t, \quad \xi=\xi(x, y, z, t), \quad \eta=\eta(x, y, z, t), \quad \zeta=\zeta(x, y, z, t),$$

where

$$\begin{aligned}
&\hat{Q}=Q/J,\\
&\hat{E}=(\xi_t/J)Q+(\xi_x/J)E+(\xi_y/J)F+(\xi_z/J)G,\\
&\hat{F}=(\eta_t/J)Q+(\eta_x/J)E+(\eta_y/J)F+(\eta_z/J)G,\\
&\hat{G}=(\zeta_t/J)Q+(\zeta_x/J)E+(\zeta_y/J)F+(\zeta_z/J)G,
\end{aligned}$$

and J is the Jacobian of transformation.

Here we assert that $\hat{E}$, $\hat{F}$, $\hat{G}$ are not the function of only $\hat{Q}$ but the function of Q and metrics, although $E=E(Q)$, $F=F(Q)$, $G=G(Q)$; for example, the conventional notation $\hat{E}=\hat{E}(\hat{Q})$ is wrong, and the notation by Chakravarthy *et al.* [2]

$$\hat{E}=\hat{E}(Q, n_t, n_x, n_y, n_z)=\hat{E}(Q, N),$$

where $n_t=\xi_t/f$, $n_x=\xi_x/J$, $n_y=\xi_y/J$, $\eta_z=\xi_z/J$,

is right. This will be refered to in the later discussion.

Details needed to apply the above mentioned schemes are fully described in [4] by Pulliam *et al.*; for example, the Jacobian matrices

$$\hat{A}\equiv\partial\hat{E}/\partial\hat{Q}, \quad \hat{B}\equiv\partial\hat{F}/\partial\hat{Q}, \quad \hat{C}\equiv\partial\hat{G}/\partial\hat{Q},$$

and the similarity transformation for the diagnonalization,

$$\hat{A}\equiv R_\xi \operatorname{diag}(a_\xi^m)R_\xi^{-1}, \quad \hat{B}\equiv R_\eta \operatorname{diag}(a_\eta^m)R_\eta^{-1}, \quad \hat{C}\equiv R_\zeta \operatorname{diag}(a_\zeta^m)R_\zeta^{-1},$$

and so on.

3. Difference Schemes

a) The Beam-Warming Scheme

Here, the Beam-Warming scheme diagonalized by Pulliam & Steger [5] in ADI algorithm is used. This algorithm has the form

$$R_\xi[I+h\delta_\xi \Lambda_\xi]N[I+h\delta_\eta \Lambda_\eta]P[I+h\delta_\zeta \Lambda_\zeta]R_\xi^{-1}\Delta\hat{Q}^n=-h[\partial_\xi \hat{E}+\partial_\eta \hat{F}+\partial_\zeta \hat{G}],$$

where $N=R_\xi^{-1}R_\eta$, $P=R_\eta^{-1}R_\zeta$, and $\Lambda_\xi=\operatorname{diag}(a_\xi^m)$, etc..

Numerical dissipation terms are added implicitly to the left hand side of this form as

$$D_{i\xi}=\varepsilon_i \Delta t J^{-1}(\nabla\Delta)_\xi J, \quad D_{i\eta}=\cdots\cdots, \quad D_{i\zeta}=\cdots\cdots,$$

and explicitly to the right hand side as

$$D_e=\varepsilon_e \Delta t J^{-1}[(\nabla\Delta)_\xi^2+(\nabla\Delta)_\eta^2+(\nabla\Delta)_\zeta^2]J.$$

On the space, the flux of right hand side is approximated by the difference of either second- or fourth-order accuracy and the left hand side by the second-order one.

b) The Yee-Harten TVD Scheme and its modified form

As the TVD schemes applied to three-dimensional problems would spend too much computational time to be solved with original nonlinear form, two linearized forms (LCI, LNI) were presented for computational efficiency and the LCI method had better convergence rate in two-dimensional case according to Yee & Harten [6]. Thus the LCI is adopted here.

An ADI form of the three-dimensionalized TVD-LCI scheme, which is the straightforward extention of the two-dimensional Yee-Harten scheme, can be expressed as

$$\begin{aligned}
&[I+\lambda^\xi\theta H^\xi_{i+1/2,j,k}-\lambda^\xi\theta H^\xi_{i-1/2,j,k}]D''\\
&\qquad=-\{\lambda^\xi[\tilde{E}^n_{i+1/2,j,k}-\tilde{E}^n_{i-1/2,j,k}]+\lambda^\eta[\tilde{F}^n_{i,j+1/2,k}-\tilde{F}^n_{i,j-1/2,k}]\\
&\qquad\quad+\lambda^\zeta[\tilde{G}^n_{i,j,k+1/2}-\tilde{G}^n_{i,j,k-1/2}]\},\\
&[I+\lambda^\eta\theta H^\eta_{i,j+1/2,k}-\lambda^\eta\theta H^\eta_{i,j-1/2,k}]D'=D'',\\
&[I+\lambda^\zeta\theta H^\zeta_{i,j,k+1/2}-\lambda^\zeta\theta H^\zeta_{i,j,k-1/2}]D=D'.
\end{aligned}$$

The numerical flux functions, which are important on this scheme, are given as follows. For example, $\tilde{E}$, is

$$\tilde{E}_{i+1/2,j,k}\equiv(1/2)[\hat{E}_{i,j,k}+\hat{E}_{i+1,j,k}+(R_\xi\Phi)_{i+1/2,j,k}],$$

where the elements of the Φ.denoted by ϕ^{m} are

$$\phi^m_{i+1/2,j,k}\equiv(1/2)\psi(a^m_{i+1/2})(g^m_i+g^m_{i+1})-\psi(a^m_{i+1/2}+\gamma^m_{i+1/2})\alpha^m_{i+1/2},$$

with the adjustment quantity for high accuracy g_1 defined by

$$g^m_i\equiv\mathrm{minmod}\,[\alpha^m_{i+1/2},\ \alpha^m_{i-1/2}].$$

Further, Roe's average [7] and artificial compression term [1] are used in order to make solutions clearer. The left hand side operator, which is the same as that of the Beam-Warming scheme except for the numerical viscosity, is also diagonalized for the

computational cost of steady state applications.

In Yee-Harten scheme $\alpha^m_{i+1/2}$ is defined by $R^{-1}(\hat{Q}_{i+1}-\hat{Q}_i)$, and it was known that this numerical flux didn't give reasonable solutions in our numerical experiment (see the latter section of this paper). Hence we have modified the numerical flux as

$$\phi^m_\kappa=(1/J_\kappa)[(1/2)\psi(a^m_\kappa)(g^m_i+g^m_{i+1})-\psi(a^m_\kappa+\gamma^m_\kappa)\alpha^m_\kappa], \quad (\kappa=i+1/2),$$

where $\alpha^m_{i+1/2}$ is defined by $R^{-1}(Q_{i+1}-Q_i)$. This modification comes from the consideration that $(\partial\hat{E}/\partial Q)\partial Q/\partial\xi$ is the better approximation of $\partial\hat{E}/\partial\xi$ than $(\partial\hat{E}/\partial\hat{Q})\partial\hat{Q}/\partial\xi$ as the flux $\hat{E}$ is the contravariant vector density of +1 wight [8].

c) The Chakravarthy-Osher TVD Scheme and its modified form

We straightforwardly extend the highly accurate one-dimensional TVD scheme [2] proposed by Chakravarthy & Osher for three-dimentional flow problems. The left hand side operator used for solving this scheme implicitly is the same as that of the Yee-Harten scheme. The numerical flux of the scheme in the right hand side is written as

$$\tilde{f}_\kappa=h_\kappa-(1-\phi)/4\{\widetilde{df}^-_{\kappa+1}\}-(1+\phi)/4\{\widetilde{\widetilde{df}}^-_\kappa\}+(1+\phi)/4\{\widetilde{df}^+_\kappa\}+(1-\phi)/4\{\widetilde{\widetilde{df}}^+_{\kappa-1}\}, \quad (\kappa=i+1/2).$$

where h is the first-order accurate flux;

$$h_{i+1/2}=(1/2)(\hat{f}_{i+1}+\hat{f}_i)-(1/2)(df^+_{i+1/2}-df^-_{i+1/2}).$$

The definition of $df^\pm$ is

where
$$df^\pm_{i+1/2}=R_{i+1/2}\sigma^\pm_{i+1/2},$$

$$\sigma^{m\pm}_{i+1/2}=a^{m\pm}_{i+1/2}\alpha^m_{i+1/2},$$

with
$$\alpha_{i+1/2}=R^{-1}_{i+1/2}(\hat{q}_{i+1}-\hat{q}_i), \qquad a^{m\pm}=(a^m\pm|a^m|)/2,$$

and flux-limited values of df are defined by

$$\widetilde{df}^-_{i+3/2}=R_{i+3/2}\widetilde{\sigma}^-_{i+3/2}, \qquad \widetilde{\sigma}^-_{i+3/2}=\text{minmod}\,[\sigma^-_{i+3/2},\ \beta\sigma^-_{i+1/2}],$$
$$\widetilde{\widetilde{df}}^-_{i+1/2}=R_{i+1/2}\widetilde{\widetilde{\sigma}}^-_{i+1/2}, \qquad \widetilde{\widetilde{\sigma}}^-_{i+1/2}=\text{minmod}\,[\sigma^-_{i+1/2},\ \beta\sigma^-_{i+3/2}],$$
$$\widetilde{df}^+_{i+1/2}=R_{i+1/2}\widetilde{\sigma}^+_{i+1/2}, \qquad \widetilde{\sigma}^+_{i+1/2}=\text{minmod}\,[\sigma^+_{i+1/2},\ \beta\sigma^+_{i-1/2}],$$
$$\widetilde{\widetilde{df}}^+_{i-1/2}=R_{i-1/2}\widetilde{\widetilde{\sigma}}^+_{i-1/2}, \qquad \widetilde{\widetilde{\sigma}}^+_{i-1/2}=\text{minmod}\,[\sigma^+_{i-1/2},\ \beta\sigma^+_{i+1/2}],$$

with "compression" parameter β. Note that $\phi=1/3$ corresponds to the third-order accurate flux, and we use it in this paper.

The above are the straightforward extension of the first approach in [2], where the

metrics with the same subscript as the term under consideration are used. Their second approach descrived as the possibility is that all terms in the numerical flux $f_{i+1/2}$ are evaluated by using the metrics $N_{i+1/2}$, but this would be quite time consuming as they state.

As the first approach did not give good solutions, we first modified this scheme so that $\alpha_{i+1/2}$ is redefined by $R^{-1}(q_{i+1}-q_i)$ and instead the terms of df, $\widetilde{df}$ and $\widetilde{\widetilde{df}}$ are multiplied by $(1/J)_{i+1/2}$, in the same way as the modification of Yee & Harten's TVD scheme. But this didn't still achieve improvement of solutions, so we further modified it as follows, in consideration of their second possibility; $a^{m\pm}$, R and R^{-1}, as well as metrics, should be evaluated at the point where the numerical flux is calculated, whatever be the value of the subscript for the term under consideration. This modified approach is rather economical than their first version.

4. Results and Discussions

1) Conditions of Numerical Experiments

Treatments of the boundary condition are similar to those of Pulliam & Steger [5]. To improve the convergence rate we also use the local time stepping $\Delta t=\Delta t_{ref}/(1+J^{1/3})$ which is proposed in [5]. The numerical computation is carried out for the ONERA-M6 wing [9]. The computational conditions are as follows. Grid used in our numerical experiment is the C-H type grid generated by the conbination of conformal mappings and shearing transformations [10]. Coarse ($89\times17\times16$) and fine ($191\times33\times24$) grids are used. Figure 1 shows the grid distribution around the wing. Notive that even the fine grid is still rough comparing with the figure of grid that was used by Yee & Harten in two-dimensional case [6]. Two typical flow problems are solved; Case 1 ($M_\infty=0.923$, $\alpha=0°$) where a strong shock wave appears remarkably and Case 2 ($M_\infty=0.84$, $\alpha=3.06°$) where a triple shock wave (weak and strong shock waves and their union) exists.

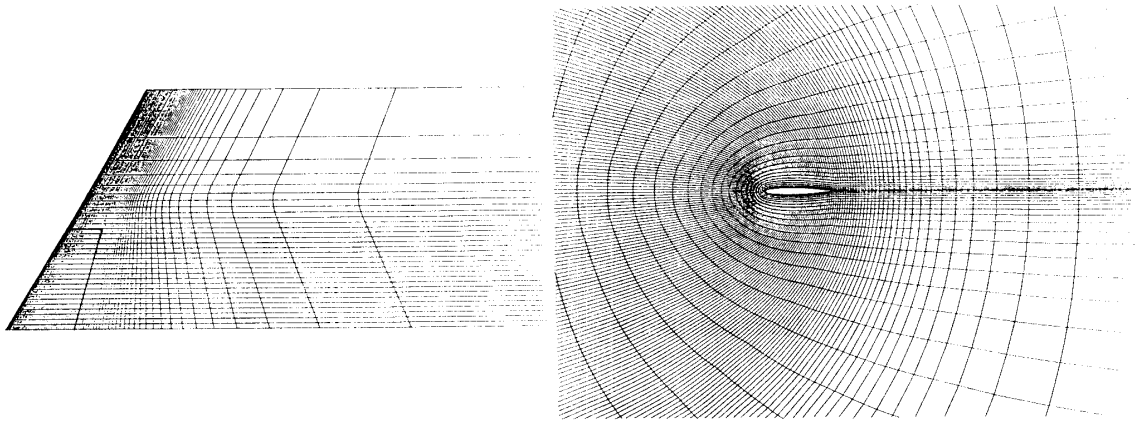

Fig. 1. Grid view around ONERA-M6 wing.

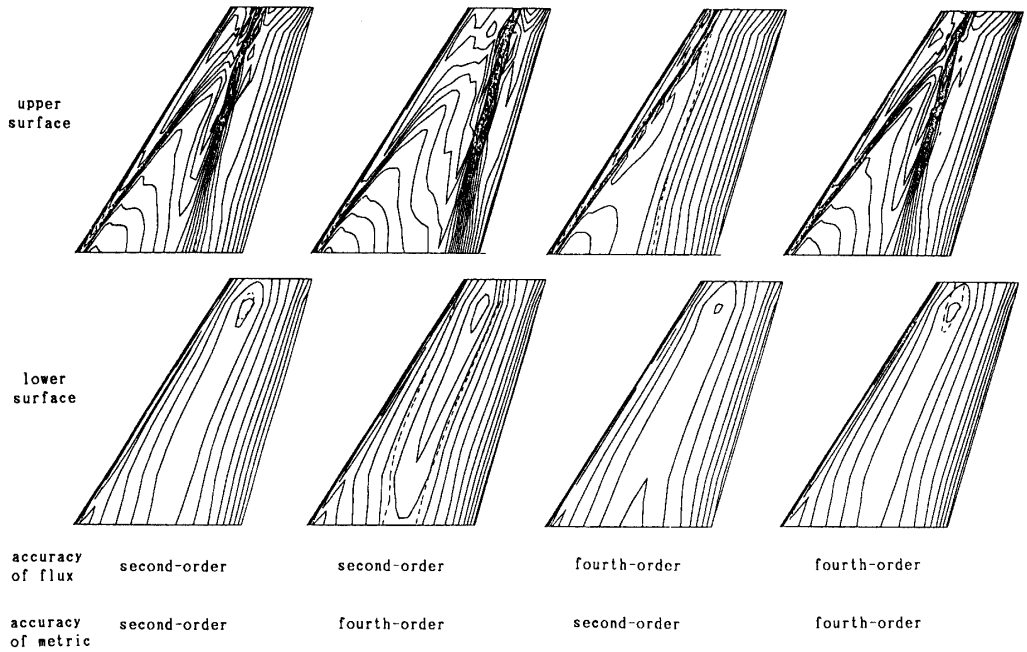

Fig. 2. Numerical experiments on accuracy of metrics (Beam-Warming scheme, $M_\infty=0.84$, $\alpha=3.06°$). Isobaric contours on wing surface.

2) Numerical Experiments on the Accuracy of Metrics

With metrics of both the second- and fourth-order accuracy on the coarse grid, Case 1 is calculated by each scheme.

a) The Beam-Warming Scheme

The two kinds of difference approximations, the second- and fourth-order accuracy, are used for the divergence of flux. Therefore there are four cases made by the combination of approximate accuracy for the metrics and divergence of flux;

Case A: second-order divergence of flux and second-order metrics
Case B: second-order divergence of flux and fourth-order metrics
Case C: fourth-order divergence of flux and second-order metrics
Case D: fourth-order divergence of flux and fourth-order metrics

The isobaric contours on the upper and lower wing surfaces are displayed in Fig. 2. Case A and D (with the same accuracy on the metrics and divergence of flux) have solutions in agreement with each other, except for small discrepancy on the behavior of numerical oscillations in the just upstream portion of remarkable strong shock waves. In the solution for Case B, the weak shock wave becomes weaker and the strong one stronger and the latter moves downstream. On the contrary, in the solution for Case C the weak shock wave grows much stronger and the strong one vanishes. The results for Case A and D of these four are most similar to the experimental data.

Now, modification for the difference of metrics is introduced by using the governing equations, where the freestream fluxes are subtracted from the original one [11]

$$\partial_t\hat{Q}+\partial_\xi(\hat{E}-\hat{E}_\infty)+\partial_\eta(\hat{F}-\hat{F}_\infty)+\partial^\zeta(\hat{G}-\hat{G}_\infty)=0,$$

These modified solutions corresponding to Case A~D are denoted by Case A′~D′ respectively. They almost agree. Especially when the oscillations by the strong shock waves are focused, one can find that Case A′ and B′ are closely similar to Case A, and Case C′ and D′ to Case D; that is, the behavior of oscillations depends on the order of the accuracy of difference approximations for the divergence of flux.

b) The Modified Yee-Harten TVD Scheme

The accuracy of the flux in this scheme corresponds to the second-order. It presents the same behavior as the Beam-Warming scheme with the second-order divergence of flux with regard to the accuracy of metrics and the improvement of solutions is also achieved by maintaining freestream.

c) The Modified Chakravarthy-Osher TVD Scheme

The accuracy of the flux in this scheme is the third-order. The behavior with regard to the accuracy of metrics and the maintenance of freestream is also same as that of the Beam-Warming scheme with the second-order divergence of flux.

From the above, it is known that there is little difference between the solutions of the second-order and fourth-order accurate divergence of the Beam-Warming scheme, and here rises the requirement that the accuracy of divergence and metrics should agree with each other. So in the following, for the Beam-Warming scheme the fourth-order accuate divergence and the same order accurate metrics are used and for the TVD schemes by Yee & Harten and Chakravarthy & Osher the second-order metrics are used, together with the maintenance of freestream.

3) Difference between Original and Modified TVD Schemes

As both the original TVD schemes by Yee & Harten and Chakravarthy & Osher did not give good solutions in Case 2, we have modified these schemes as was descrived in the previous section. The differences of solutions in Case 2 on the fine grid between the original and modified Yee-Harten schemes and between the original and modified Chakravarthy-Osher schemes are clearly shown in Fig. 3 and Fig. 4 respectively. In the solutions by both the original TVD schemes the triple shock waves observed in experiments do not appear, but instead only the strong shock waves emerge, while the modified TVD schemes capture the triple shock waves clearly. In addition, in Case 1 where a remarkable shock wave is observed in the experiments, the original and modified schemes give corresponding solutions with each other.

The reason of the fact that both the original TVD schemes capture the strong shock waves but miss the weak shock waves, we consider, comes from that the relation $\partial\hat{E}/\partial\xi=(\partial\hat{E}/\partial\hat{Q})\partial\hat{Q}/\partial\xi$ etc. is wrong. This relation does not contain the differences of metrics in $\hat{E}$, and more precise expression must be

$$\partial\hat{E}/\partial\xi=(\partial\hat{E}/\partial Q)\partial Q/\partial\xi+(\partial\hat{E}/\partial N)\partial N/\partial\xi,$$

where N denotes certain metric, since $\hat{E}=\hat{E}(Q, N)$ as was previously mentioned. Probably the second term not estimated in the schemes causes the numerical error where the variations of metrics are large, and this is amplified because of some interpolations—usual Roe's average—when eigenvalues at midpoints are calculated.

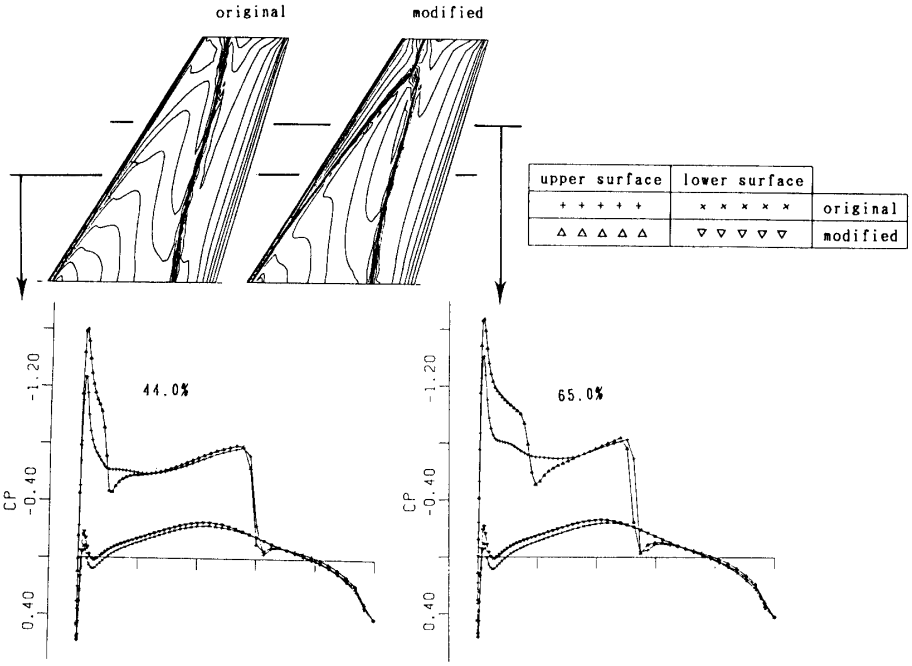

Fig. 3. Comparison between original and modified Yee-Harten schemes (M_∞=0.84, α=3.06°, fine grid). Isobaric contours on upper wing surface and Cp distributions.

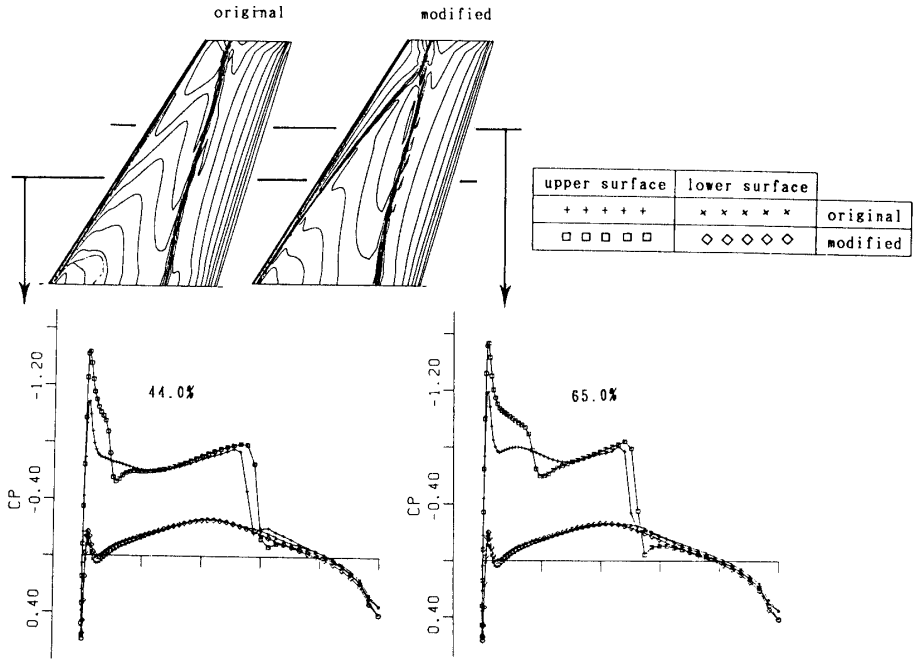

Fig. 4. Comparison between original and modified Chakravarthy-Osher schemes (M_∞=0.84, α=3.06°, fine grid). Isobaric contours on upper wing surface and Cp distributions.

4) Comparison of Schemes

Here three kinds of schemes, the Beam-Warming scheme, the modified Yee-Harten TVD scheme and the modified Chakravarthy-Osher TVD scheme, are chosen as objects of comparison.

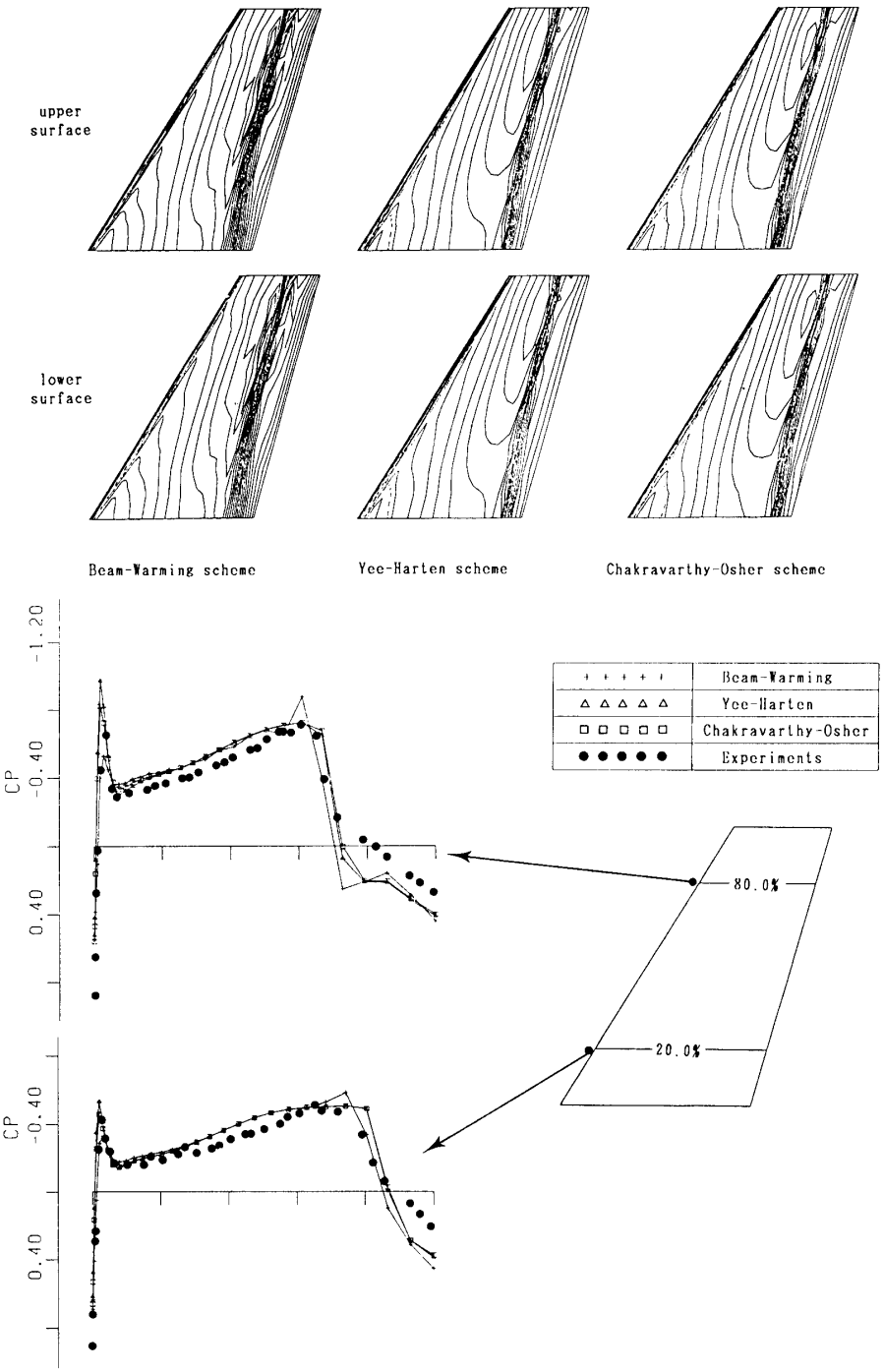

Fig. 5. Comparison among schemes (M_∞=0.923, α=0.0°, coarse grid).
(a) Isobaric contours on wing surface.
(b) Cp distributions on wing surface.

Case 1. In this case it is known a strong shock wave appears remarkably. Figure 5 and Fig. 6 show the Cp distributions by each scheme on the coarse and fine grids respectively. It is remarkable the solutions by both the TVD schemes coincide very well with each other. It is clearly observed that the solution by the Beam-Warming scheme has the numerical oscillations in the upstream and downstream of the shock

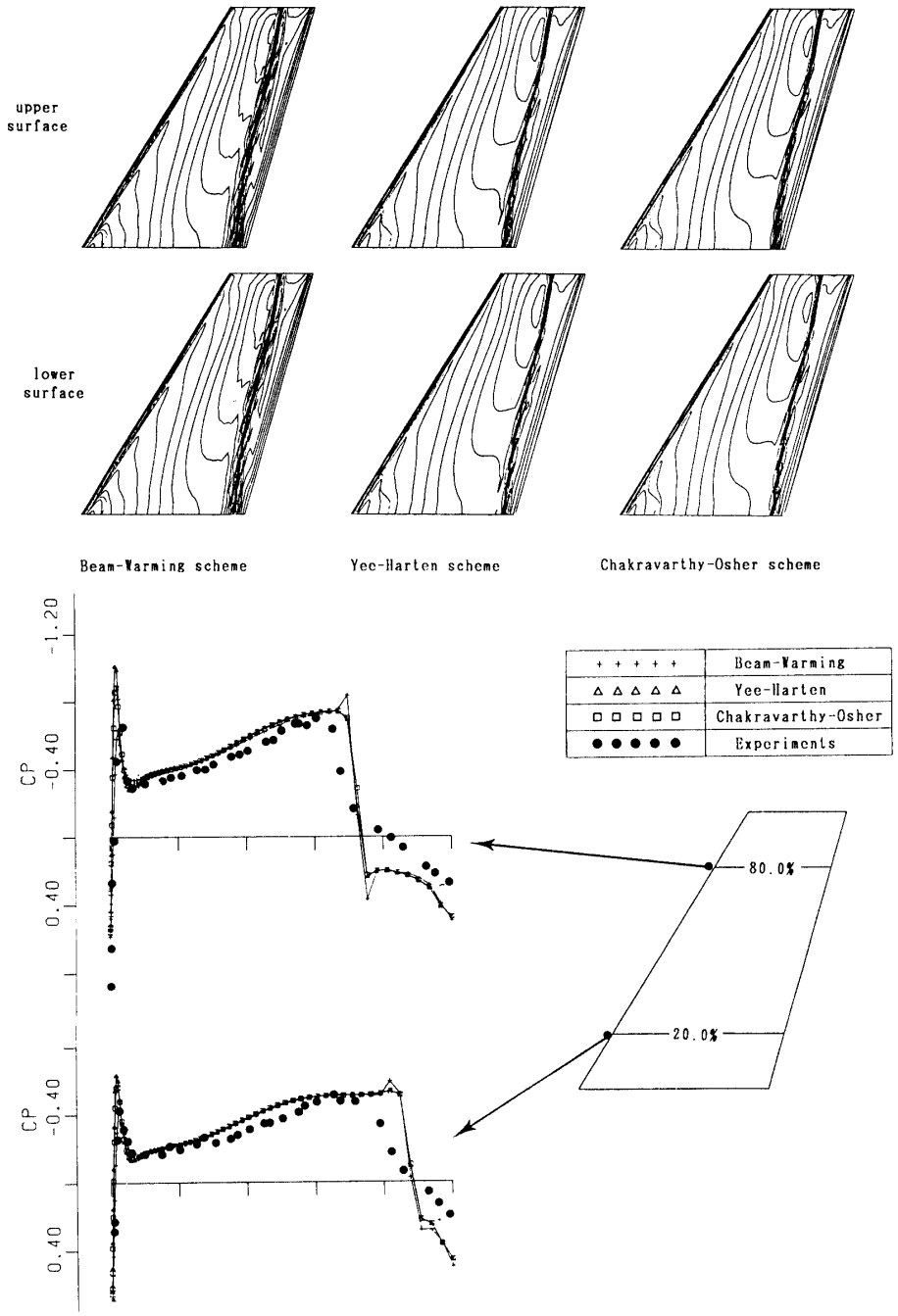

Fig. 6. Comparison among schemes (M_∞=0.923, α=0.0°, fine grid).
(a) Isobaric contours on wing surface.
(b) Cp distributions on wing surface.

wave and those by the TVD schemes, on the other hand, have very few oscillations. On the coarse grid, the shock wave by the Beam-Warming scheme is located more upstream than those by the TVD schemes. On the fine grid, the shock wave by each scheme becomes stronger and clearer than that on the coarse grid, it moves downstream, the location of shock waves all agree with each other, and also the expansion around the leading edge becomes clearer. As to the leading edge expansion the modified Yee-Harten TVD scheme captures it most clearly, the modified

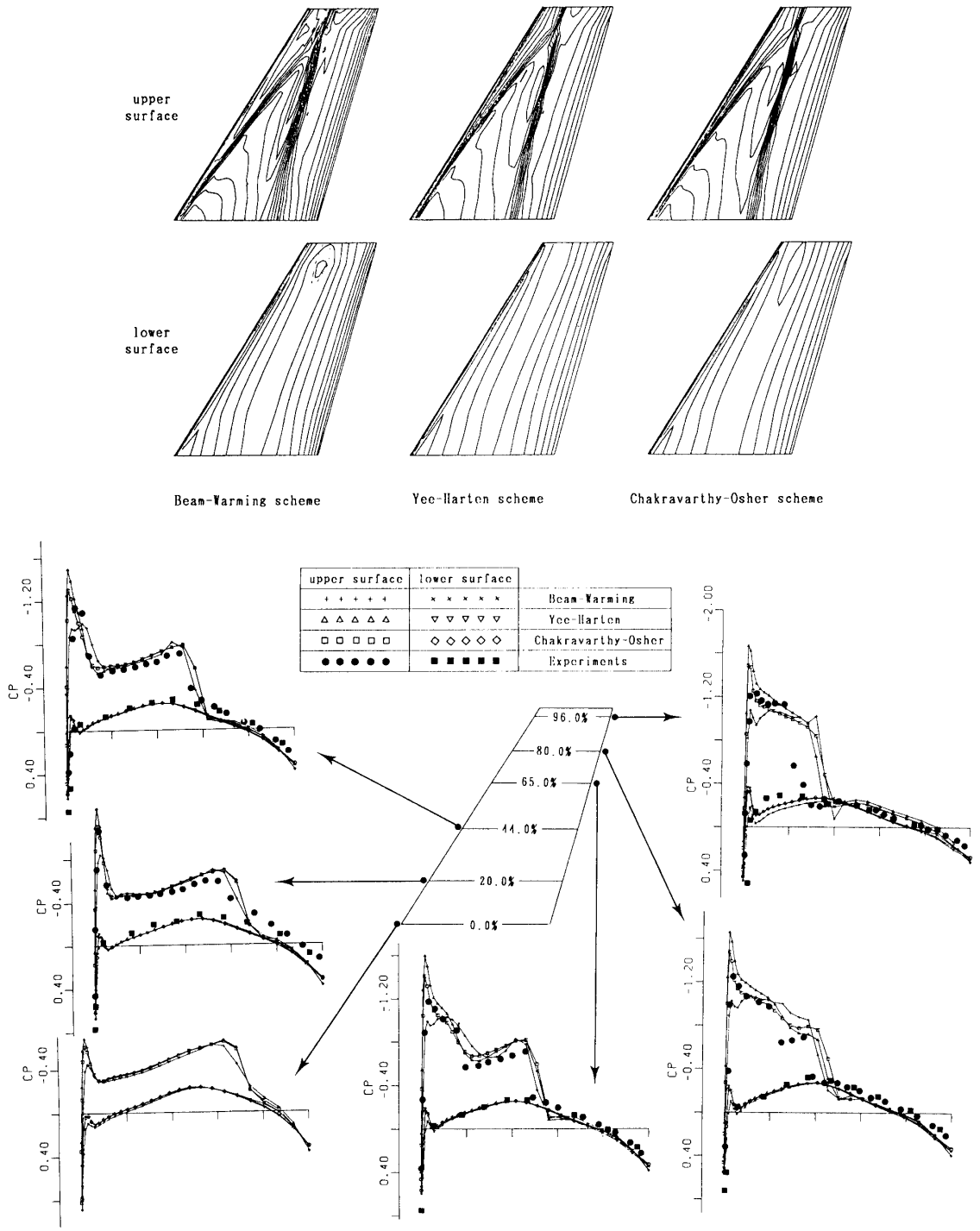

Fig. 7. Comparison among schemes (M_∞=0.84, α=3.06°, coarse grid).
(a) Isobaric contours on wing surface.
(b) Cp distributions on wing surface.

Chakravarthy-Osher TVD scheme secondly. Although solutions on the coarser grid show better agreement with experimental data [10] which contain viscous effect, solutions on the finer grid must be closer to the true inviscid solution of Euler equations.

We may say that the solutions by TVD schemes are better than that by

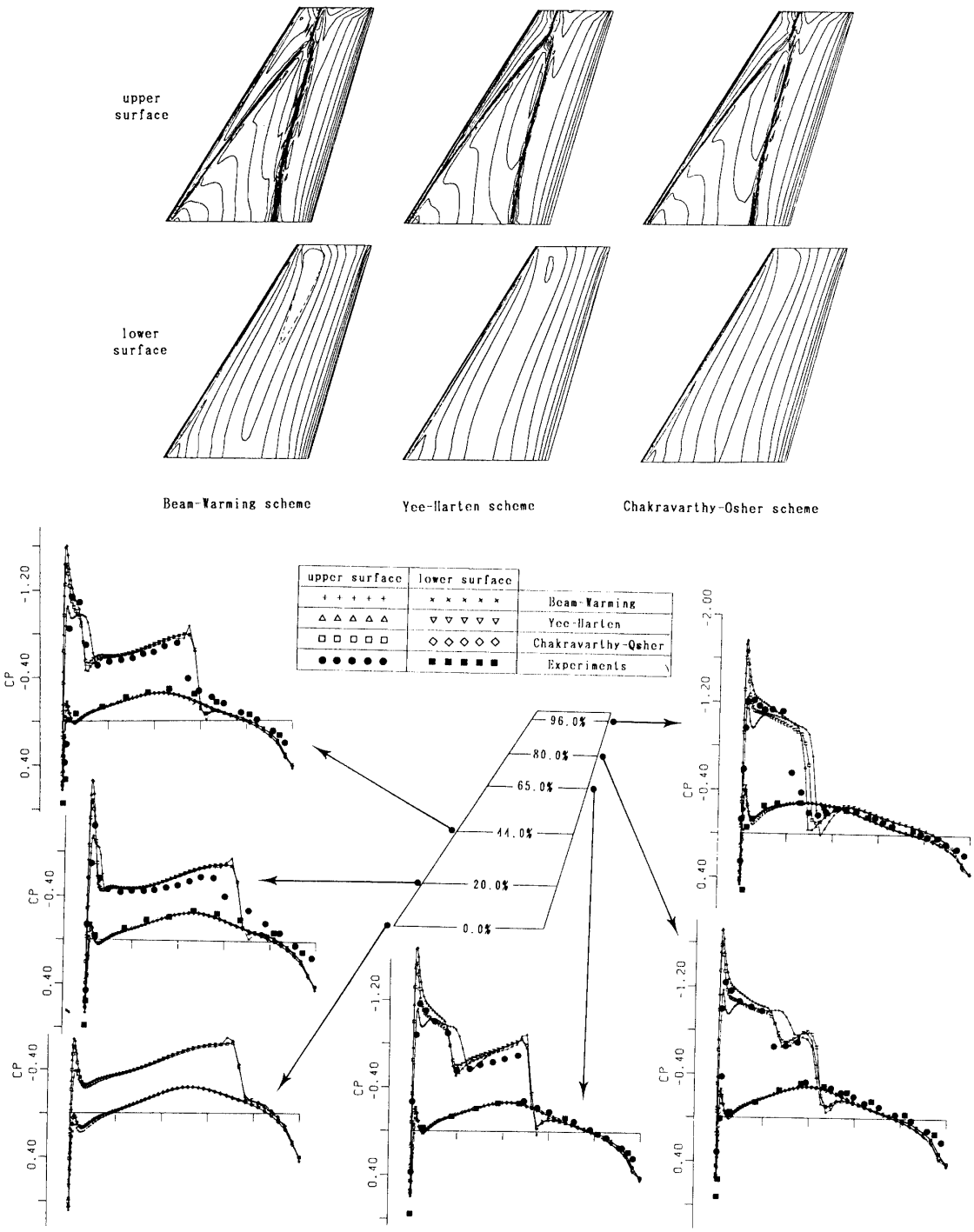

Fig. 8. Comparison among schemes (M_∞=0.84, α=3.06°, fine grid).
(a) Isobaric contours on wing surface.
(b) Cp distributions on wing surface.

Beam-Warming scheme in this case.

Case 2.. In this case it is well known that a triple shock wave exists, and the characteristic features of the schemes become more clearly evident than in Case 1. Figure 7 and Fig. 8 show the Cp distributions by each scheme on the coarse and fine

grids respectively. As was expected, the weak and strong shock waves and leading edge expansion by each scheme become clearer on the finer grid. The solutions by both TVD schemes almost agree, except for the strength of leading edge expansion and weak shock waves and the location of united shock waves of weak and strong shocks.

As to the strong shock wave (see results on semi-span locations of 20%, 44%, and 65%), its behavior is almost same as in Case 1, except that its location is not so much affectd by the fineness of grid. The Beam-Warming scheme produces oscillations near the strong shock wave but the modified TVD schemes very few ones. About the fineness of grid, the strong shock wave by the Beam-Warming scheme on the coarse grid is a little front of that on the fine grid, while the locations of those by the TVD schemes are almost same on both the coarse and fine grids.

As to the leading edge expansion and weak shock wave (see results on semi-span locations of 44% and 65%), the modified TVD schemes capture its tendency in experiments [9] much better than the Beam-Warming scheme. Both the TVD schemes capture the leading edge expansion more excessively than the experiments and the weak shock wave just at the same position as experiments, while the Beam-Warming scheme captures the former less sufficiently and the latter more downstream than the experiments. The ability of capturing the former by each scheme is the same order as in Case 1.

As to the united shock waves (see results on semi-span location of 96%), on the fine grid their locations lie more upstream and are nearer to the experiments than on the coarse grid, contrary to strong shock waves in Case 1. The reason would be that on the finer grid the forward weak shock waves become stronger and clearer, and this cause the united location of weak and strong shock waves to move ahead. The nearest shock wave to the experiments is that by the modified Yee-Harten TVD scheme, the next nearest is that by the modified Chakravarthy-Ocher TVD scheme. Further, the Cp distributions on 80% semi-span location (at a little distance to the root direction from the position where the weak and strong shock waves are united) by both the TVD schemes are more similar to the experiments than that by the Beam-Warming scheme.

In this case, the solutions on the fine grid show the better agreement with the experiments than those on the coarse grid, and especially the modified TVD schemes give an excellent agreement. We may say that the solutions by the modified TVD schemes are much better than that by the Beam-warming scheme, but it cannot be decided which of the two is closer to the true Euler solution.

5) Convergence History and Computing Time

Convergence history of L_2 norm of residual for every scheme in Case 2 on the coarse grid is presented in Fig. 9. The computing time required to reach a steady state is shown in Table 1. Here "steady state" is defined as the state when the L_2 norm of residual decreases by order 10^{-3} from the starting one. The Yee-Harten TVD scheme requires more in both the computing time for an interation and number of iterations than the Beam-Warming scheme, so the total CPU time required for the steady state is 2.4 times as much as the latter. The Chakravarthy-Ocher TVD scheme has the

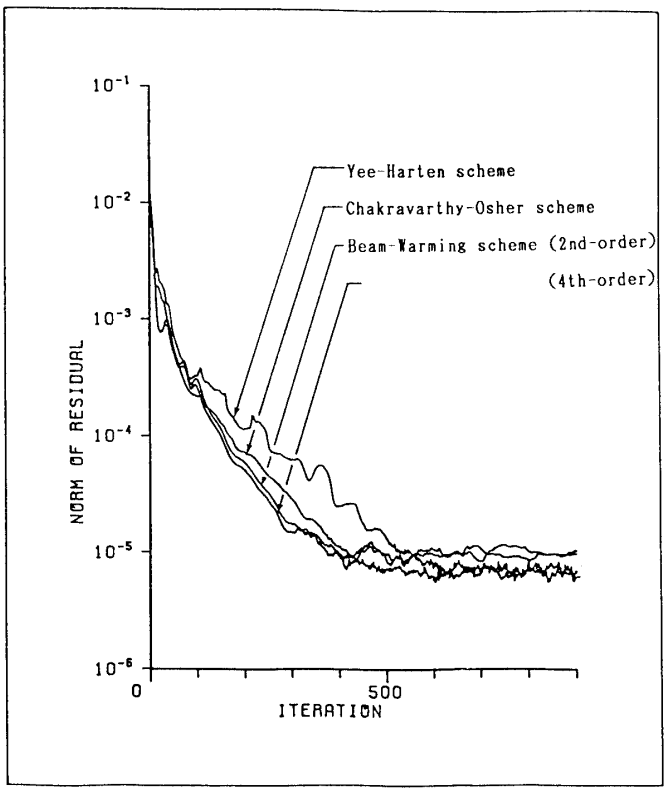

Fig. 9. Convergence history.

Table 1. Comparison of Computing Time

scheme	time for an iteration	number of iterations	total CPU time
Yee-Harten	1.75	1.38	2.4
Chakravarthy-Osher	2.23	1.05	2.3
Beam-Warming (2nd order)	1.0	1.0	1.0
(4th order)	1.03	0.95	1.0

almost same convergence history as the Beam-Warming scheme but consumes much computing time, so the total CPU time is 2.3 times. These computing data were obtained on FACOM M-380.

Conclusions

The modification of the recent TVD schemes with regard to treatment of metrics has been presented, and further, the estimation for the TVD schemes and the conventional Beam-Warming scheme has been performed by comparing the computational results for the three-dimensional flows about the ONERA-M6 wing together with the experimental data. Consequently our modified TVD schemes have been proved to be reasonable when applied to the three-dimensional Euler equation in general curvilinear coordinates and moreover the characteristics of each scheme

have been captured. On the accuracy of metric, it was verified for each scheme that it should be made agree with accuracy of fluxes, otherwise modification of maintaining freestream should be used.

The Beam-Warming scheme yields a moderate solution with comparatively short computing time. On the other hand, our modified TVD schemes yield excellent solutions with very few numerical oscillations for even remarkable strong shock waves and high ability of capturing the leading edge expansion and weak shock waves. In general, the TVD schemes have the defects of much computing cost, and further we must take care of computing the numerical flux in curvilinear coordinate system, i.e., the original TVD schemes are not applicable to three-dimensional problems because they capture strong shock waves clearly but miss the weak shock waves. It may be said that the numerical simulation by using the TVD schemes has just started and many interesting subjects will be left in the future.

In addition this study has been done as a part of the software package development in National Aerospace Laboratory.

REFERENCES

[*1*] Yee, H. C., Warming, R. F. & Harten, A.: J. Comp. Phys. **57** (1985) 327–360.
[*2*] Chakravarthy, S. R. & Osher, S.: AIAA paper 85–0363.
[*3*] Beam, R. & Warming, R. F.: J. Comp. Phys. **22** (1976) 87–110.
[*4*] Pulliam, T. H. & Chaussee, D. S.: J. Comp. Phys. **39** (1981) 347–363.
[*5*] Pulliam, T. H. & Steger, J. L.: AIAA paper 85–0360.
[*6*] Yee, H. C. & Harten, A.: AIAA paper 85–1513.
[*7*] Roe, P. L.: J. Comp. Phys. **43** (1981) 357–372.
[*8*] Ogawa, S. & Ishiguro, T.: Preprint of I.S.C.F.D.-Tokyo, (1985) 931–942.
[*9*] Schmitt, V. & Charpin, F.: AGARD AR-138 (1979).
[*10*] Ishiguro, T.: NAL TR-731 (1982).
[*11*] Pulliam, T. H. & Steger, J. L.: AIAA Journal **18** (1980) 159–167.

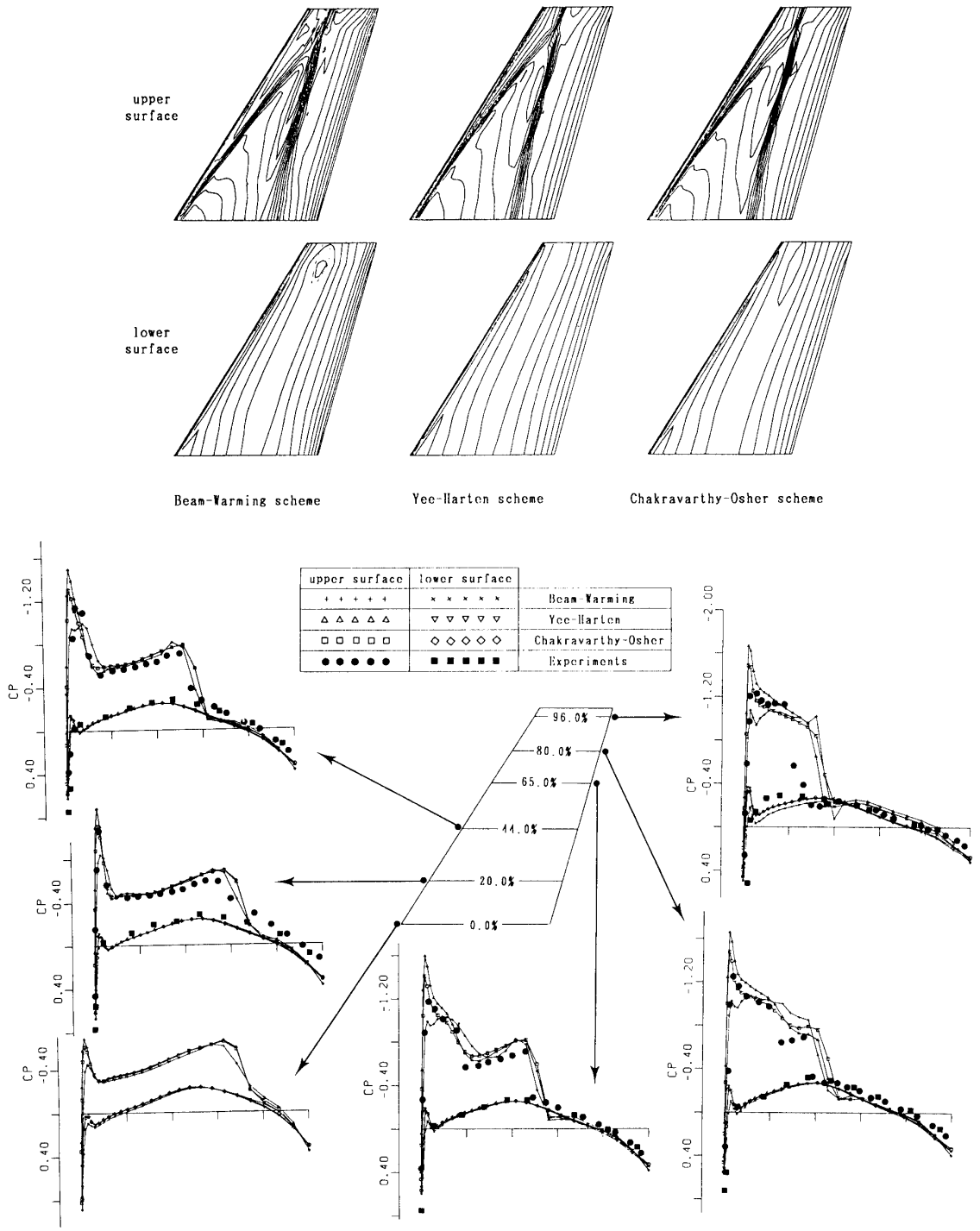

Fig. 7. Comparison among schemes (M_∞=0.84, α=3.06°, coarse grid).
(a) Isobaric contours on wing surface.
(b) Cp distributions on wing surface.

Chakravarthy-Osher TVD scheme secondly. Although solutions on the coarser grid show better agreement with experimental data [10] which contain viscous effect, solutions on the finer grid must be closer to the true inviscid solution of Euler equations.

We may say that the solutions by TVD schemes are better than that by